HHS Public Access

Author manuscript

Fire Saf J. Author manuscript; available in PMC 2015 November 10.

Published in final edited form as:

Fire Saf J. 2012 July ; 51: 110–119.

Evaluation of Criteria for the Detection of Fires in Underground Conveyor Belt Haulageways

Charles D. Litton and **Inoka Eranda Perera**

National Institute for Occupational Safety and Health (NIOSH) Office of Mine Safety and Health Research (OMSHR) 626 Cochrans Mill Road, PO Box 18070 Pittsburgh, PA 15236

Abstract

Large-scale experiments were conducted in an above-ground gallery to simulate typical fires that develop along conveyor belt transport systems within underground coal mines. In the experiments, electrical strip heaters, imbedded ~5 cm below the top surface of a large mass of coal rubble, were used to ignite the coal, producing an open flame. The flaming coal mass subsequently ignited 1.83-meter-wide conveyor belts located approximately 0.30 m above the coal surface. Gas samples were drawn through an averaging probe located approximately 20 m downstream of the coal for continuous measurement of CO, CO_2, and O_2 as the fire progressed through the stages of smoldering coal, flaming coal, and flaming conveyor belt. Also located approximately 20 m from the fire origin and approximately 0.5 m below the roof of the gallery were two commercially available smoke detectors, a light obscuration meter, and a sampling probe for measurement of total mass concentration of smoke particles. Located upstream of the fire origin and also along the wall of the gallery at approximately 14 m and 5 m upstream were two video cameras capable of both smoke and flame detection. During the experiments, alarm times of the smoke detectors and video cameras were measured while the smoke obscuration and total smoke mass were continually measured.

Twelve large-scale experiments were conducted using three different types of fire-resistant conveyor belts and four air velocities for each belt. The air velocities spanned the range from 1.0 m/s to 6.9 m/s. The results of these experiments are compared to previous large-scale results obtained using a smaller fire gallery and much narrower (1.07-m) conveyor belts to determine if the fire detection criteria previously developed (1) remained valid for the wider conveyor belts. Although some differences between these and the previous experiments did occur, the results, in general, compare very favorably. Differences are duly noted and their impact on fire detection discussed.

Introduction and Background

Fires in underground mines represent a significant and potentially catastrophic hazard. Constant vigilance is one of the keys to minimizing this hazard and its possible consequences. Conveyor belt entries are of particular concern for a variety of reasons. First, conveyor belt entries often extend for thousands of meters with only periodic inspections,

Disclaimer: The findings and conclusions in this paper are those of the authors and do not necessarily represent the views of the National Institute for Occupational Safety and Health.

often at long intervals corresponding to the beginning/ending of shift changes. Because fires can develop rapidly along these entries, the need for some type of automatic fire detection and warning system becomes readily apparent. Second, some mines may need to use the conveyor entry as an intake entry to supply additional fresh air for a working section. Because the toxic combustion products and smoke from a fire travel with the ventilation, the possibility for rapid and significant contamination of a working section greatly increases the hazard potential, thus placing a greater burden on the fire detection and warning system. Third, the conveyor belt represents an essentially continuous source of fuel running the length of an entry. Previous experiments, along with actual conveyor belt fire incidents, indicate the potential for rapid flame spread along the conveyor belt surfaces (2, 3, 4). During rapid flame spread, tremendous heat may be generated along with potentially lethal levels of CO and smoke. Large fires such as these also alter an entry's resistance to airflow (5), thus producing dramatic effects on the mine ventilation flow patterns which can, in turn, adversely impact evacuation and control measures.

Fires within conveyor belt entries typically develop in three stages. First, loose coal from the conveyor belt deposits along a conveyor idler or electrical cable. If the idler begins to overheat due to friction or if there is an electrical fault in a cable, the heat generated is dissipated within the loose coal, producing low-temperature smoldering combustion. As the temperature of the loose coal increases, fuel vapors from the smoldering coal eventually ignite, producing the second stage of visible flame that will begin to spread across the surfaces of the coal. When the flames from the coal fire impinge upon the surfaces of the conveyor belt for a sufficient period of time, then the surface of the conveyor belt ignites and the flames begin to spread. This is the third stage of fire development. When the heat release rate from the burning conveyor belt is of sufficient intensity, then rapid flame spread along the surface of the conveyor belt can occur, often producing disastrous consequences.

In the early 1990s, large-scale experiments were conducted to simulate this fire scenario and the data was used to develop a set of guidelines for fire detection systems (1). A major constraint of these guidelines was the criterion that actual detection and subsequent alarm of the fire detection system must occur just prior to ignition of the conveyor belt. This constraint is necessary because once the conveyor belt is ignited, the potential for rapid flame spread and large fires producing copious levels of toxic gases and smoke increases dramatically. If detection/alarm is not achieved before belt ignition, the chances for successful evacuation and control can be significantly diminished.

These guidelines have been incorporated into Title 30, Code of Federal Regulations (30 CFR), regarding the installation and use of atmospheric monitoring systems when airflow through a belt entry is used to ventilate a working section (6). In addition, effective January 1, 2010, 30 CFR, Part 75, removed the requirement for point-type heat sensors along conveyor belt entries and replaced this with a requirement for CO sensors or their equivalent. In addition to these regulatory changes, recommendations from the recent Technical Advisory Panel on the Use of Belt Air and the Composition and Fire Retardant Properties of Belt Materials in Underground Coal Mining has recommended the widespread use of smoke sensors for early warning fire detection in conveyor belt haulageways (7). Lastly, there has been an increase in the use of wider conveyor belts for transport of coal,

leading to concern relevant to whether the use of wider belts and higher belt air ventilation velocities impacts the fire detection guidelines for spacing and alarm levels.

To test the validity of the previous guidelines and the possible impact of wider belts on the fire detection process, large-scale experiments using wider belts were conducted in an above ground Fire Suppression Facility (FSF) at the Lake Lynn Laboratory operated by the National Institute for Occupational Safety and Health (NIOSH). The FSF has a cross-sectional area roughly 55% greater than the one used in the prior experiments (11.7 m^2 compared to 7.53 m^2). Tests were conducted at air velocities of 1.0 m/s, 2.0 m/s, 4.1 m/s, and 6.9 m/s—air velocities that span the range of those typically found in underground mines. The nomographs in Figures 7 and 8 of Ref. 1 allow for the determination of CO and smoke sensor alarm levels as a function of the entry cross-sectional area and the air velocity for sensor spacing of 300 and 600 m. Using the nomographs for the 300-m sensor spacing, the respective CO alarm levels are found to be 9 ppm at 1.0 m/s, 5 ppm at 2.0 m/s, 3 ppm at 4.1 m/s, and 1 ppm at 6.9 m/s; for smoke sensors, the required alarm levels are optical densities (OD) of 0.044 m^{-1} at air velocities of 1.0 m/s and 2.0 m/s, and 0.022 m^{-1} at air velocities of 4.0 m/s and 6.9 m/s.

In the sections that follow, the data acquired during the current experiments will be presented and analyzed using the detection criterion of alarm just prior to belt ignition as previously discussed and described in depth in Ref. 1. This will be done in order to assess the continued validity of this criterion or, if necessary, to modify this previous criterion.

Experimental

Figure 1 shows photographs of the NIOSH Fire Suppression Facility, including the pile of coal rubble, the conveyor haulage frame, conveyor belt, and locations of the gas averaging probe and other detection equipment. The FSF is constructed of masonry block walls, a steel roof, and a concrete floor. The walls and roof are coated with a fire-resistant cementitious coating. The cross-sectional area of the tunnel exit is 11.7 m^2.

For these experiments, air was forced through the gallery using a variable speed axi-vane fan at four (4) discrete air velocities—1.0 m/s, 2.0 m/s, 4.0 m/s, and 6.9 m/s. In order to straighten the airflow, ten 0.09-m-thick wood panes were placed in front of the fan. The distance of the fan to the middle of the coal bed was 25 m. Three different types of fire-resistant conveyor belts were used, known generically by their primary polymer component as styrene butadiene rubber (SBR), polyvinyl chloride (PVC), and neoprene (NP). Testing all three conveyor belts at each of the four air velocities resulted in a total of twelve (12) experiments.

To ignite the coal, six electrical strip heaters measuring 0.921 × 0.038 m and separated by approximately 0.3 m were imbedded within the pile of coal rubble, approximately 5 cm below the top surface of the coal. The strip heaters were rated at 1500 W at 120 V, producing a maximum surface temperature of 650 °C (1200 °F). All heaters were turned off after the coal fire ignited the belt sample and the belt fire had been well-developed in the ignition area (typically after 15 minutes of the belt fire). A 1.8-m-wide by 1.5-m-length belt was placed on the rollers of the conveyer belt structure (21 m long and 1.5 m wide), hanging

towards the coal bed where the strip heaters were fixed. The coal bed consisted of about 350 kg of 1-cm to 5-cm pieces of Pittsburgh seam coal (38.6% volatility). The distance from the top surface of the coal pile to the bottom surface of the belt was about 5-10 cm.

The gallery was instrumented with thermocouples to measure the gas temperature. A thermocouple was fixed at the center of the belt to measure the temperature of the fire at the belt ignition (1.5 m from the middle of the coal bed). Seven thermocouples were connected to the roof from the conveyer belt frame, starting at the coal pile every 1.5 m, to measure the average gas temperature at the exit stream. A smoke and gas sample averaging probe was positioned at the tunnel exit, downstream of the coal pile 19.8 m from the coal bed. This probe was constructed from a 5-cm-diameter steel pipe, and had four inlet ports spaced along the vertical height of the tunnel to measure the smoke and the gas concentration at the exit stream. The gas samples were analyzed for O_2, CO, and CO_2. An Interscan Corporation RM series Rackmount Monitor[1] CO analyzer with a sensitivity of 0 to 100 ppm was used to measure the CO. An inline filter was used to eliminate interference due to other gases, dust particles, and aerosols. An Infrared Industries IR-208[1] was used to analyze CO_2 and O_2.

In addition to the gas analysis, two smoke detectors were located near the roof, 19.4 m from the coal pile, to measure the smoke density. The two photoelectric smoke detectors were an ASD FILTREX-F[1] and the diode laser detector PINNACLE[1]. Both sensors were fixed to a common fire panel channeled to a computer through an electronic processer. A smoke obscuration meter was also placed 19.4 m downstream from the coal pile, 40 cm from the tunnel roof, to measure the light obscuration at a wavelength of 635 nm. A gas sample was extracted from a point just beyond the obscuration meter and flowed to a TSI DustTrak[1] for simultaneous measurement of smoke mass concentrations. An Axonx[1] video smoke and fire detection system was also used to monitor the visible smoke levels and the progress of the developing fires. Two Axonx video monitors were fixed upstream of the coal fire at 13.4 m and 4.5 m, allowing the developing fire to be viewed from two different vantage points.

The outputs of the thermocouples and the analyzers were connected to a 60-channel microprocessor and transmitted to a National Instruments[1] data logger to view the output data. For the initial nine experiments, data were obtained at 10-s intervals, and for the final three experiments at an air velocity of 6.9 m/s at 2-s intervals. Experiments were also video recorded.

Even though the experimental setup was very similar to the setup in the previous experiments (1), some differences are worth noting:

- In the previous setup, the above-ground fire gallery cross-sectional area was 7.5 m^2, compared to 11.7 m^2 for the current setup.

- The heating of the coal pile was direct in the current experiment as opposed to a step-wise heating in the previous experiment.

[1]Mention of company names or products does not constitute endorsement by the National Institute for Occupational Safety and Health.

- The width of the belt is greater in the current experiments (1.83 m) than that of the previous experiment (1.02 m).

Results

Fire Detection Data and Analysis

Once power was supplied to the electrical strip heaters, the mass of coal began to heat, producing smoke for a period of time before finally erupting in flame. Once flaming occurred, the fire intensity increased until the coal flames ignited the conveyor belt material. During these stages of fire growth, the smoke and CO also increased as time progressed. In the twelve experiments conducted, the average time (measured from the moment power was supplied to the electrical heaters) to observe the first glimpse of smoke from the smoldering coal was 8 minutes. From the time the heaters were energized, the average time for the coal to burst into flame was 24 minutes, or 16 minutes after smoldering began. These smoldering time periods are comparable to results previously reported (1).

As the fire intensity increases, the fire hazards also increase, especially subsequent to belt ignition, since it is during this time that rapid flame spread can occur. As discussed previously, the primary constraint on the fire detection system is to detect a developing fire prior to belt ignition, or as quickly as possible thereafter before the onset of rapid flame spread can begin. Adopting this constraint, the detection data is best analyzed by comparing the sensor alarm times with the times at which belt ignition occurred. In order to do this—assuming a maximum spacing of 300 m between consecutive fire sensors—an average travel time for the bulk average CO or smoke to travel with the ventilation air velocity a distance equal to one-half of the sensor spacing (150 m), plus an average sensor response time of 60 s (1 min), must be added to the alarm concentration appearance time measured just downstream of the developing fire. The use of a travel time corresponding to a distance equal to one-half the sensor spacing (rather than the maximum sensor spacing) is consistent with the criteria developed previously (1), where the probability for the origin of a fire along a conveyor belt is the same for any point between two consecutive sensor locations. In addition, the standard deviation (or uncertainty) in the time to belt ignition is 8.32 minutes for these experiments, sufficiently greater than the additional travel time that would be calculated on the basis of the maximum spacing. With an uncertainty of 8.32 minutes, all air velocities greater than 0.30 m/s would require less time to travel the additional distance of one-half the sensor spacing.

The total time, t_a, needed for a sensor to alarm is the time, t_{conc}, it takes for the fire to produce the required bulk average CO or smoke alarm concentration (as measured from the instant of flaming coal ignition) at a given air velocity plus the travel time, t_t, for this concentration of CO or smoke to travel. On average, one-half of the distance between two consecutive sensors (150 m) plus the sensor response time, t_R, is taken for convenience to be 60 seconds. For these experiments, the sum of the two latter times—travel time plus sensor response time ($t_t + t_R$)—which must be added to the bulk average alarm concentration appearance time, t_{conc}, at the indicated air velocities, are as follows:

1. $V_0 = 1.0$ m/s, $t_t + t_R = 210$ s (3.50 min),

2. V_0 = 2.0 m/s, $t_t + t_R$ = 135 s (2.25 min),
3. V_0 = 4.1 m/s, $t_t + t_R$ = 98 s (1.63 min), and
4. V_0 = 6.9 m/s, $t_t + t_R$ = 82 s (1.37 min).

Table 1 and Figure 2 display the estimated average times of alarm for a CO sensor at the specified alarm thresholds and spaced at 300 m. The solid curve of Figure 2 is the time to belt ignition, t_{BI}, and represents a value for comparison with the detection times. Points falling above this line mean that the CO detection system failed to detect the developing fire prior to belt ignition, while points falling on or below this line mean that the CO detection system was able to detect the fire just prior to belt ignition. In general, the CO detection appears to satisfy the detection criterion reasonably well. While there is some scatter in the data and there are some detection times greater than the time to belt ignition, the overall average was 28.2 s (0.47 min) *before* belt ignition. These results are encouraging relative to the continued use of Ref. 1 as a guide for specifying fire detection requirements using CO sensors.

It is also of considerable interest to examine the data obtained for smoke sensors. In these experiments, it was not possible to measure a bulk average optical density (OD) for the smoke due to the physical limitations of the gas sample averaging probe and the need to keep the connecting lines of this probe free of contamination. However, estimates of the bulk average OD levels, and thus the times at which the smoke reaches the alarm points, can be obtained using the relationships given by Equations (9) and (10) from Ref. 1, along with the expressions for the CO and smoke production parameters in Figures 3 and 4 of this paper. For CO, the ppm CO is given by

$$ppm \quad CO = B_{CO} \bullet (Q_F / V_0 A_0) \quad (1)$$

where Q_F is the coal fire heat release rate, kW,

V_0A_0 is the product of ventilation air velocity and entry cross-sectional area, m^3/s, and

B_{CO} is the CO production constant = $4.80 \cdot \exp(-0.175V_0)$. The smoke OD is given by

$$OD = B_{OD} \bullet (Q_F / V_0 A_0) \quad (2)$$

where

$$B_{OD} \quad \text{is the smoke production constant} = 0.037 \bullet exp(-0.100V_0)$$

For detection at distances far-removed from the fire origin, gases and smoke mix almost completely with the ventilation airflow so that bulk average concentrations are the quantity of interest. Clearly, the length of the large-scale tunnel limits the ability to reproduce this mixing so, instead, a gas averaging probe is used to obtain the average gas concentrations. Because of losses of smoke particles in the length of tubing connecting the remote analyzers to the gas averaging probe, no average smoke obscuration (optical density, OD) data is obtained and estimates of the smoke obscuration were calculated using the empirical relationships above. The bulk average smoke optical density can then be estimated from the

measured bulk average CO by combining Equations (1) and (2) and the respective expressions for the CO and smoke production constants, to yield

$$OD = (ppm \quad CO) \bullet (\mathrm{B}_{OD}/\mathrm{B}_{CO}) = (ppm \quad CO) \bullet 0.00771 \bullet exp\,(0.075\mathrm{V}_0) \quad (3)$$

Using this expression, the bulk average smoke OD can be estimated from the measured bulk average CO. For each experiment, the bulk average smoke OD was then plotted as a function of time, with the times to reach the required smoke alarm levels tabulated as previously done for CO. In addition, the optical density at smoke sensor alarm was measured for the smoke sensors using the smoke obscuration meter located near the roof at the end of the fire tunnel. The average smoke optical density at the moment of smoke sensor alarms was found to be 0.0257 m^{-1}, a value that falls between the OD alarm levels specified using the nomographs of Ref. 1. To determine what effect the measured OD at which smoke alarm occurs might have on the detection time, this data is also included in Table 2 (column 5) and in Figure 3.

Just as in the previous Figure 2 for CO, the smoke detection system has satisfied the detection criterion if the time falls either on the solid line or below it. The results indicate that like the data for CO, it is apparent that the criteria previously developed (1) remain valid. It is also worth noting that the average detection time using alarm values from the previous study (1) is *2.66 minutes before* the belt ignites. For the detection times using the measured average OD at alarm of 0.0257 m^{-1}, detection occurs an average of *5.23 minutes before* the belt ignites.

It must be noted that the above data and estimates for CO and smoke optical density were for bulk average quantities—the quantities that would exist far downstream of a developing fire after there is essentially complete mixing of the fire combustion products with the ventilation airflow. Closer to the fire origin, stratification of the combustion products near the roof of an entry occurs, with concentrations decreasing as the distance from the roof increases (8). In general, the recommendation for product of combustion fire sensors has always been to locate the sensors approximately 0.3 m to 0.5 m below the roof in order to take advantage of any stratification that may occur should the fire occur not too far upstream of the sensor location. Sensors located near the roof can be more efficient and provide earlier detection should a fire occur upstream and relatively close to the sensor location. In general, the degree of stratification decreases as the air velocity increases, with maximum stratification expected to occur when no airflow exists. In these experiments, two commercially available smoke sensors were located near the end of the tunnel, one on either side of the conveyor belt frame and approximately 0.5 m below the roof of the FSF. A light obscuration meter and the intake port for the smoke mass monitor (DustTrak[1]) were also located at the same horizontal and vertical positions, approximately along the centerline of the conveyor belt frame. This was done to obtain additional information on the smoke properties of optical density and mass concentration not only on a continuous basis but, in particular, to measure these quantities at the moment of smoke sensor alarm.

Table 3 and Figure 4 show the alarm times obtained for the smoke sensors and for the Axonx video smoke/flame detection system. Just as for the data on bulk average

concentrations presented above, all alarm times are measured from the moment of flaming ignition of the coal (t = 0.0) so that negative times in Table 3 and Figure 4 are best expressed as “minutes before flaming ignition of the coal”.

On average, the smoke sensors alarmed 4.32 minutes before flaming coal ignition, while the Axonx video smoke system alarmed 9.80 minutes before flaming coal ignition. It is also worth noting that smoke sensor alarms were slightly earlier at the higher air velocities (4.1 m/s and 6.9 m/s) than at the lower air velocities (1.0 m/s and 2.0 m/s) (4.44 minutes and 4.20 minutes, respectively, before flaming coal ignition). The earlier detection by the Axonx system may be due to a higher sensitivity of the equipment or to the location of the video cameras that provided direct viewing of the fire origin.

It is also of interest to estimate the CO concentration near the roof, based on the measured optical density, as the fire develops. Since no CO sensor was available to co-locate alongside the smoke obscuration meter near the roof at the exit of the tunnel, estimates of the approximate roof level of CO were made (in a manner similar to that used for estimating bulk average smoke optical density) by solving Equations (1)–(3) for ppm CO in terms of smoke OD, yielding the following expression:

$$ppm \quad CO = OD \bullet (\mathrm{B}_{CO}/\mathrm{B}_{OD}) = OD \bullet 129.73 \bullet exp(-0.075\mathrm{V}_0) \quad (4)$$

Assuming that the smoke and CO stratify in the same manner (8) (a reasonable assumption), then Equation (4) provides a convenient means for estimating the CO concentration near the roof. Using equation (4), the CO near the roof can be plotted as a function of time using the measured values of smoke optical density. As for the bulk average data, the time at which the alarm concentration is measured (or estimated) is shown in Table 4 and Figure 5. In a manner similar to that observed for the smoke sensor alarms, the estimated alarm times for a CO sensor near the roof often occur prior to flaming ignition of the coal. In this experiment, on average, the estimated roof CO alarm occurred *8.13 minutes before* belt ignition. Even accounting for the additional travel time for the bulk average CO, this average roof CO alarm time is significantly more rapid, indicating the benefit of locating sensors near the roof in order to take advantage of the stratification that may occur at short distances downstream of the fire.

Fire Intensities, Growth Rates, and CO Production

In these experiments, the flaming coal fire grew at a slower rate than in the previous experiments. The most probable reason for this is the different manner used to bring the electrical strip heaters to their maximum surface temperature mentioned previously, although the moisture content or minor differences in the physical/chemical properties of the coal could have also been contributing factors. As a result of this slower growth rate, the average time to reach belt ignition was longer by approximately 2 minutes (16.24 ± 8.32 min compared to 14.25 min from the previous study in Ref. 1). The slower growth rates are displayed in Figure 6, where the average rate at each air velocity is plotted versus the air velocity. Even though these growth rates are lower than those previously measured, qualitatively the rates increased as the air velocity increased, a trend also found in the prior

experiments (1, 9). More detailed information on the effect of air velocity obtained in this study can be found in Ref. 10.

Because the coal fire intensities were somewhat lower for these experiments compared to the previous experiments, the time for the belt to ignite also increased. These average times to belt ignition are shown in Figure 7 at each of the air velocities and compared to the times previously measured. It is worth noting that the average time to belt ignition for the current experiments is very similar to that previously observed, with a least squares analysis yielding a slope (2.55) very close to that previously measured (2.45) and an intercept (5.5) also very close to the previous value of 8.0.

From the previous study (1), the coal fire intensity (heat release rate, Q_F) divided by the ventilation air velocity (V_0), at the time of flaming ignition of the conveyor belt was found to have an average value of 24.26 kJ/m ± 8.75, indicating that the fire was still relatively small when the belt ignited. It is also of interest to compare the values of this ratio obtained in the current experiments to this previous average value.

The heat release rate can be calculated using the combustion gases of CO_2 and CO using Equation (5):

$$Q_{TOTAL} = [Hc/k_{CO2}] \times M_{CO2} + [(Hc - k_{CO} H_{CO})/k_{CO}] \times M_{CO} \quad (5)$$

where,

H_C = total (net) heat of combustion of the fuel, kJ/g,

H_{CO} = heat of combustion of CO, 10.1 kJ/g,

k_{CO2} = stoichiometric yield of CO_2 , g/g, = 3.67 X_C where X_C is the carbon mass fraction,

k_{CO} = stoichiometric yield of CO, g/g, =2.33 $X_{C,}$

M_{CO2} = generation rate of CO_2 from the fire, g/s = 1.97×10^{-3} $V_0 A_0$ ΔCO_2

M_{CO} = generation rate of CO from the fire, g/s = 1.25×10^{-3} $V_0 A_0$ ΔCO

V_0 = air velocity, m/s,

A_0 = entry cross section area, 11.7 m^2

ΔCO_2 = CO_2 produced by fire, ppm

ΔCO = CO produced by fire, ppm

Substitution of the above parameters for Equation (5) gives

$$Q_{TOTAL} = \left[2.30 \times 10^{-2} [Hc/k_{CO2}] \Delta CO_2 + 1.46 \times 10^{-2} [(Hc - k_{CO} H_{CO})/k_{CO})] \Delta CO\right] \times V_0 \quad (6)$$

The data generated from Equation (1) are shown in Table 5, where the ratio of fire heat release rate to ventilation air velocity at belt ignition was found to have an average value of 16.36 kJ/M ± 4.09, approximately 32.6% lower than the previously measured value. However, because of the fact that in some of the experiments, the estimated time for

detection of CO (Table 1 and Figure 2) occurred after belt ignition, it is instructive to also calculate this ratio at the time of detection, yielding an estimate of the fire intensity when detection occurs. These ratios are shown in column 3 of Table 4, with an average value of 18.46 ± 5.22, also lower than the previously measured value of 24.26.

Equation (1) provides a convenient expression to estimate the level of CO produced from a flaming coal fire as a function of the fire's heat release rate. It is of interest to compare the bulk average concentration of CO measured to the concentration predicted at the moment of belt ignition. The results of these computations are shown in Table 5, Figure 8, and Figure 9. While some of the measured CO concentrations are in good agreement with the predicted levels in Figure 8, several of the experiments were not in such good agreement with some measured levels being higher by factors of around 2 and some lower by roughly 50%.

In general there is good agreement between the measured and estimated values for CO at belt ignition for experiments conducted at the lower air velocities. For experiments conducted at the higher air velocities, the measured values are, on the average, greater than the predicted values by about 2.0 to 2.5 ppm. This means that the method used to estimate these lower CO alarm levels tends to occur on the side of increased safety. However, these higher measured CO levels at the higher air velocities would indicate that there may be some flexibility to increase the CO alarm threshold at the higher air velocities.

Analysis and Alarm Tables

Equations (11) and (19) from the previous study (1) can be combined so that the product of CO alarm level, CO_A, and entry cross-sectional area, A_0, becomes a function only of air velocity, V_0, for a fixed sensor spacing, ℓ_S, and sensor response time, t_R. The result is given by the expression

$$CO_A \bullet A_0 = (B_{CO} \bullet \alpha_{COAL}/V_0)\,(t_D - t_R - \ell_S/120V_0) \quad (7)$$

where t_D is the total time available for detection (14.25 min from the previous study (1) and 16.24 min from the present data),

t_R = 60 s (1 min), and

ℓ_S = 304.8 m.

Since the total quantity of air flowing in an entry, Q_0, equals the product V_0A_0, equation (7) can be used to determine the product $CO_A \bullet Q_0$ as a function of air velocity. By setting the value of CO_A to the discrete, allowed values of 1 ppm to 10 ppm, the respective allowed values of the air quantity may then be determined for each of the 10 CO alarm levels as a function of the air velocity. Dividing Q_0 by the respective value of V_0 yields a resultant value of entry cross-sectional area, A_0, and the allowable values of Q_0 can then be plotted or tabulated as a function of entry cross-sectional area at each CO alarm level.

In a similar manner, equations (12) and (20) from the previous study (1) can be combined to yield a similar expression for smoke optical density alarm levels, OD_A, in inverse meters. The result is

$$OD_{\mathrm{A}} \bullet \mathrm{A}_0 = (\mathrm{B}_{\mathrm{D}} \bullet \alpha_{COAL}/\mathrm{V}_0)\,(\mathrm{t}_{\mathrm{D}} - \mathrm{t}_{\mathrm{R}} - \ell_{\mathrm{S}}/120\mathrm{V}_0) \quad (8)$$

Assuming three smoke optical density alarm levels, OD_A, of 0.044 1/m, 0.033 1/m, and 0.022 1/m, plots or tables of allowable air quantities as a function of entry cross-sectional area at each alarm level can also be constructed.

Results of these computations for both CO and smoke sensors and for both measured times to belt ignition (14.25 min and 16.24 min) are displayed in Tables 6-17 for the spacing of 304.8 m.

Discussion and Recommendations

The data and analysis presented in the previous sections indicate that the detection criterion previously developed and presented in great detail in Ref. 1 remains valid for wider belts, higher air velocities, and larger entry cross sections. With the exception of two very long times to ignite the belt (and these due more to the condition of the coal rather than the belt material), there was no apparent effect of belt material on the ignition of the different belts. It was found that the alarm levels for both CO and smoke optical density are functions not only of the coal fire heat release rate, but also of the ventilation air velocity and the entry cross-sectional area. In these experiments, the relatively large cross-sectional area of the fire gallery (11.7 m^2) played a role in dictating the alarm levels of the CO and smoke sensors. However, using higher air velocities in entries with smaller cross-sectional areas would tend to increase the alarm levels, meeting the detection criteria previously developed (1). For instance, at an air velocity of 4.064 m/s in an entry of 9.29 m^2, the indicated alarm level for CO sensors spaced at 304.8-m intervals is 4.0 ppm, and in an entry with a cross-sectional area of 7.43 m^2 the indicated CO alarm level would increase to 5.0 ppm. These numbers point to the fact that the sensor alarm levels necessary for adequate fire detection in conveyor belt haulageways will tend to decrease as the air quantity (product of air velocity and entry cross-sectional area) increases. This would mean that in mines with larger entry cross sections, lower sensor alarms would be required than in mines with smaller entry cross-sections—a result primarily of increased dilution of the combustion products by the ventilation airflow.

It is important to note that CO sensors may not operate reliably at the lowest alarm levels due to inherent sensor limitations or to normal fluctuations in the background levels of CO for a particular application. In these cases, excessive electronic noise within the sensor or fluctuations in the background CO level may produce false, or nuisance, alarms that can degrade confidence in the system. In situations such as these, the limiting parameter will generally be the quantity of air flowing within an entry. As a guide, Tables 6 – 17 show the CO and smoke alarm levels required for a range of cross-sectional entry areas and air quantities.

It is also worth noting that, in general, smoke sensors, especially those approved by an appropriate testing laboratory such as Underwriters Laboratory or Factory Mutual, will generally be able to tolerate the smoke optical density alarm levels of 0.022 m^{-1} and 0.044 m^{-1} because part of the approval process requires measurement of false alarm rates and

minimum measurable optical densities. Thus, approved smoke sensors can be expected to perform reliably relative to inherent false alarms attributable primarily to the electronics. However, suspended mine dusts can have a negative impact on smoke detector performance, and some consideration should be given to smoke sensors that are designed to perform in harsh, dusty environments with a minimum of maintenance.

References

1. Litton CD, Lazzara CP, Perzak FJ. Fire Detection for Conveyer Belt Entries. Bureau of Mines Report of Investigations. 1991; 9380:23.
2. Perzak FJ, Litton CD, Mura KE, P Lazzara C. Hazards of Conveyor Belt Fires. Bureau of Mines Report of Investigations. 1995; 9570:33.
3. Luzik SJ, Desautels LA. Coal Mine fires Involving Track and Belt Entries 1970-1988. Bureau of Mines Report of Investigations. 1990:09–323-90.
4. U.S. Department of Labor. Mine Safety and Health Administration. Report of Investigations. 2007:46–08801.
5. Litton CD, DeRosa M, Li JS. Calculating Fire-Throttling of Mine Ventilation Airflow. Bureau of Mines Report of Investigations. 1987; 9076:21p.
6. Title 30—Mineral Resources; Chapter 1—Mine Safety and Health Administration. Department of Labor, Subchapter O—Coal Mine Safety and Health; part 75—Mandatory Safety Standards—Underground Coal Mines; 2010.
7. Mutmansky J, Brune J, Calizaya F, Mucho T, Tien J, Weeks J. Final Report of the Technical Study Panel on the Utilization of Belt Air and the Composition and Fire Retardant Properties of Belt Materials in Underground Coal Mining. 2007
8. Conti, RS.; Litton, CD. Effects of Stratification on Carbon Monoxide Levels from Mine Fires; Proceedings of the 6th US Mine Ventilation Symposium; 1993. Chapter 73
9. Egan MR. Impact of Air Velocity on the Development and Detection of Small Coal Fires. Bureau of Mines Report of Investigations. 1993; 9480:15p.
10. Perera IE, Litton CD. Impact of Air Velocity on the Detection of Fires in Conveyor Belt Haulageways. Fire Technology. 2011 DOI: 10.1007/s10694-011-0228.

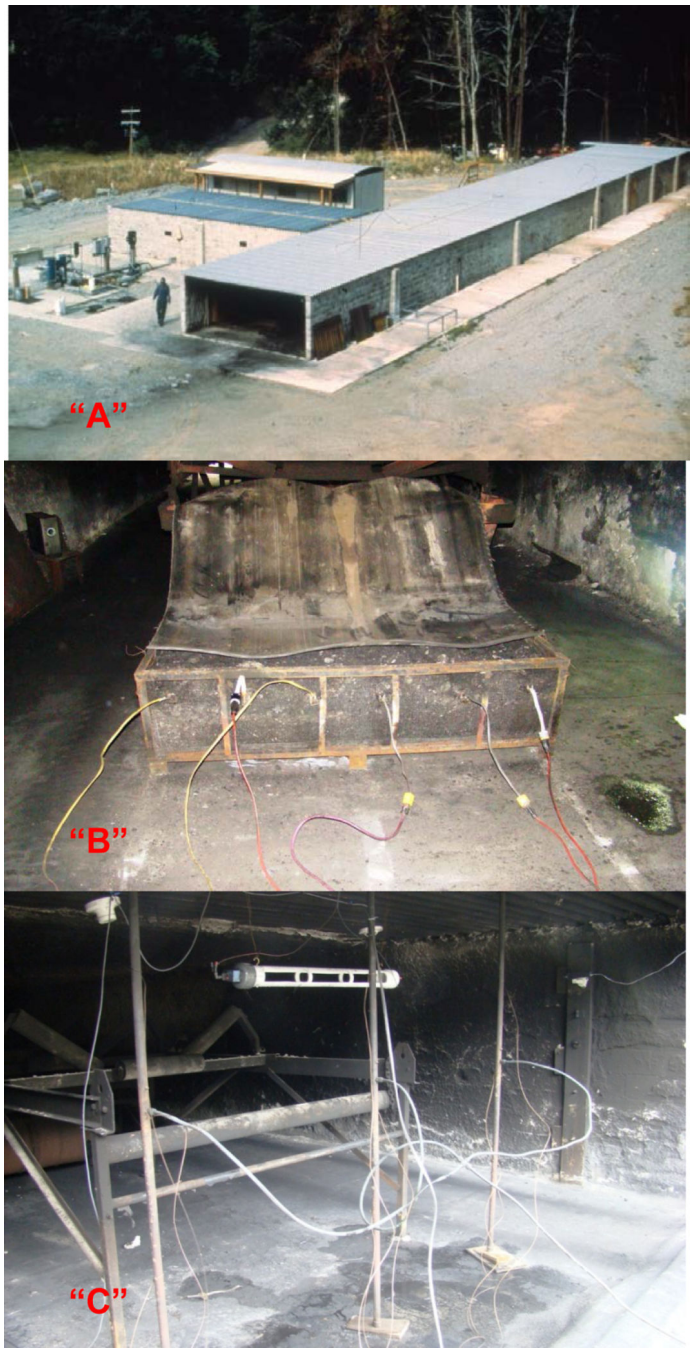

Figure 1.
Photographs showing the fire suppression facility "A", the rubbleized coal with strip heaters and conveyor belt "B", and the gas sampling and other instrumentation at the exit of the fire suppression facility "C".

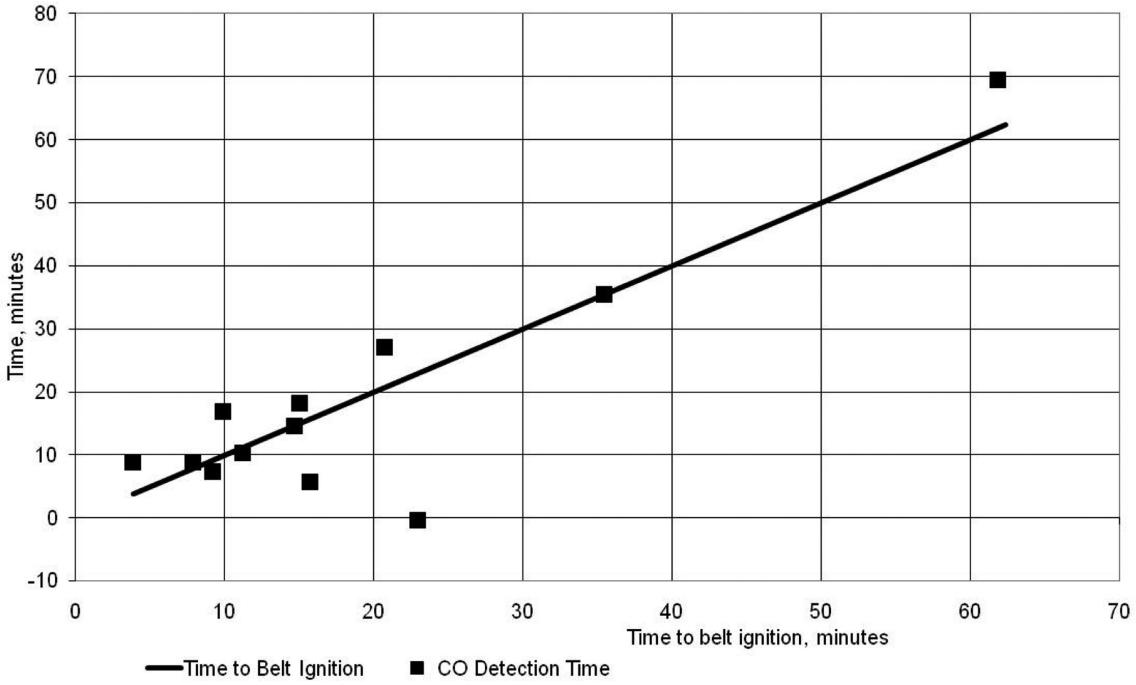

Figure 2.
Estimated CO detection times compared to the measured belt ignition times.

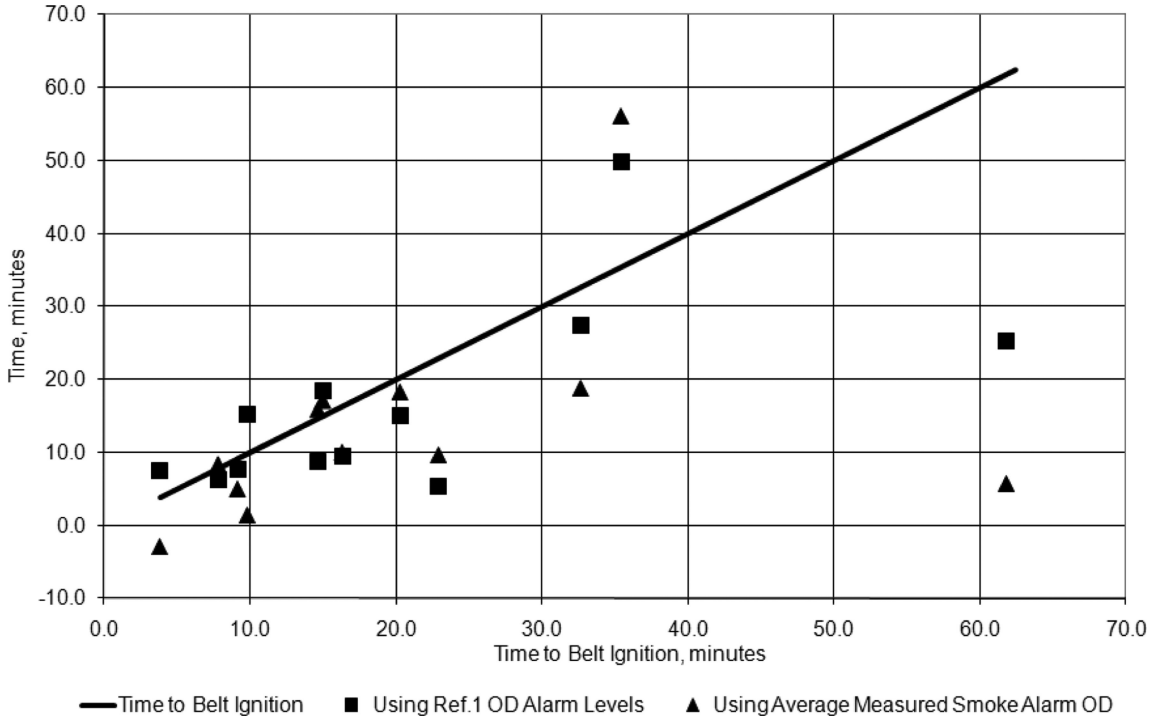

Figure 3.
Graph of estimated smoke sensor alarm times relative to the time of belt ignition.

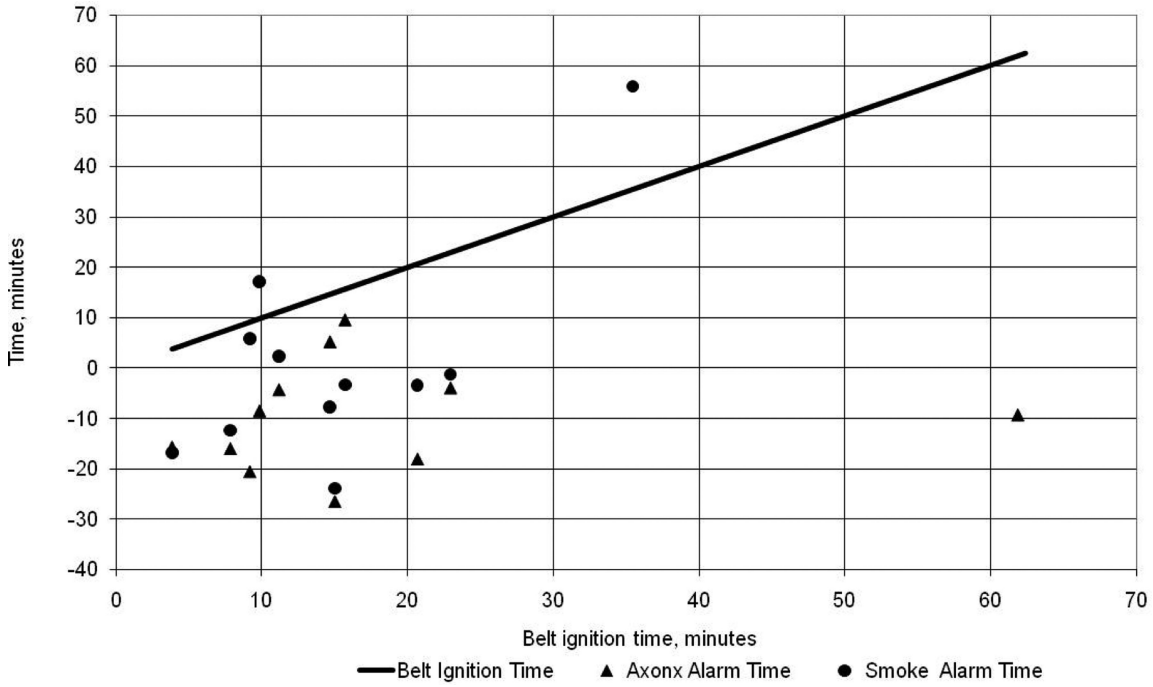

Figure 4.

Smoke sensor, Axonx, and coal ignition times (zero times) in comparison to the belt ignition times. Zero time corresponds to the time of flaming coal ignition.

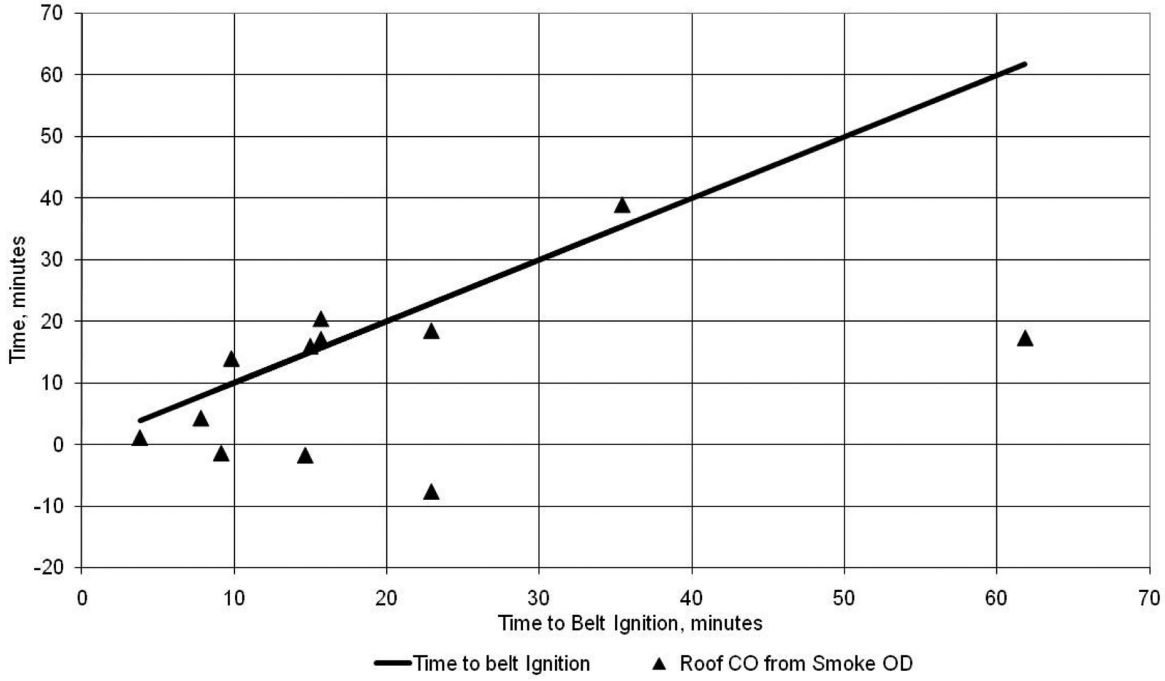

Figure 5.
Roof CO alarm times estimated from the smoke optical density.

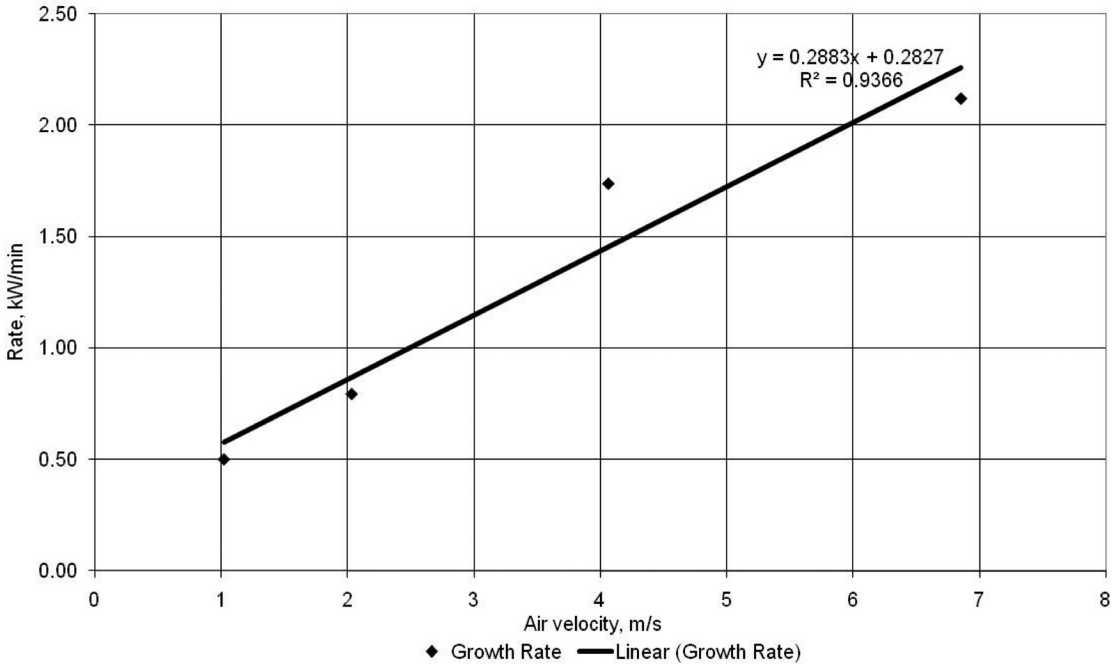

Figure 6.

Measured average coal fire growth rates from the time of flaming coal ignition to the time of ignition of the conveyor belts.

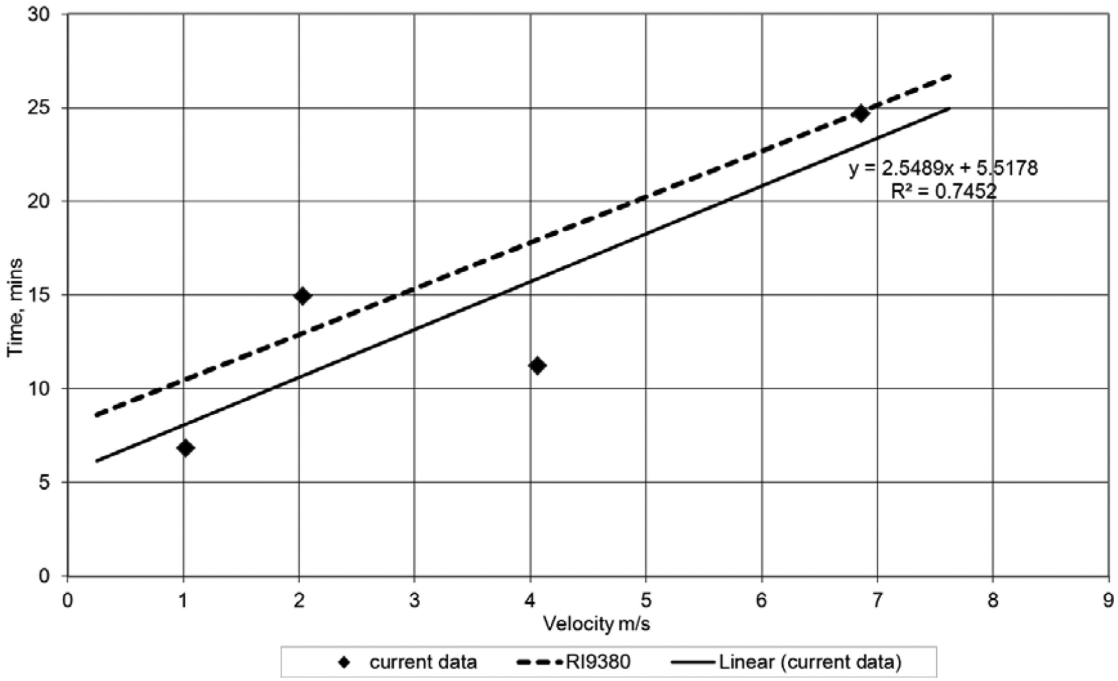

Figure 7.
Variation of the average belt ignition time with the air velocity- A comparison between the current data and the data from the previous study (1).

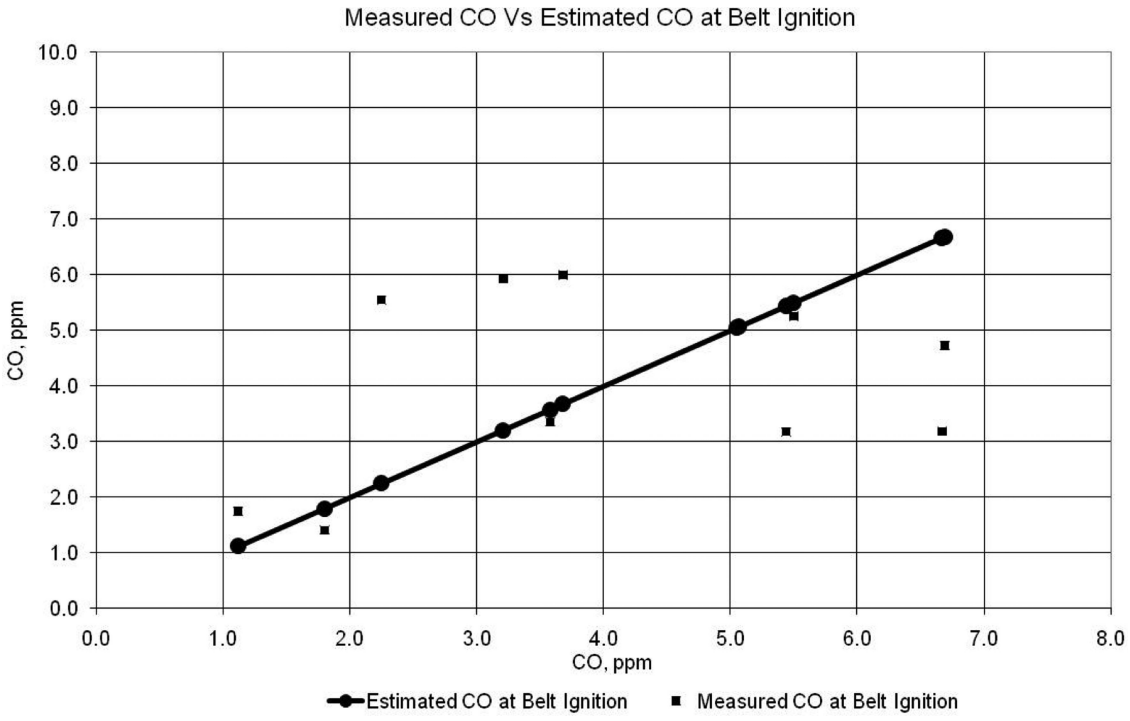

Figure 8.
Measured CO and estimated CO at belt ignition.

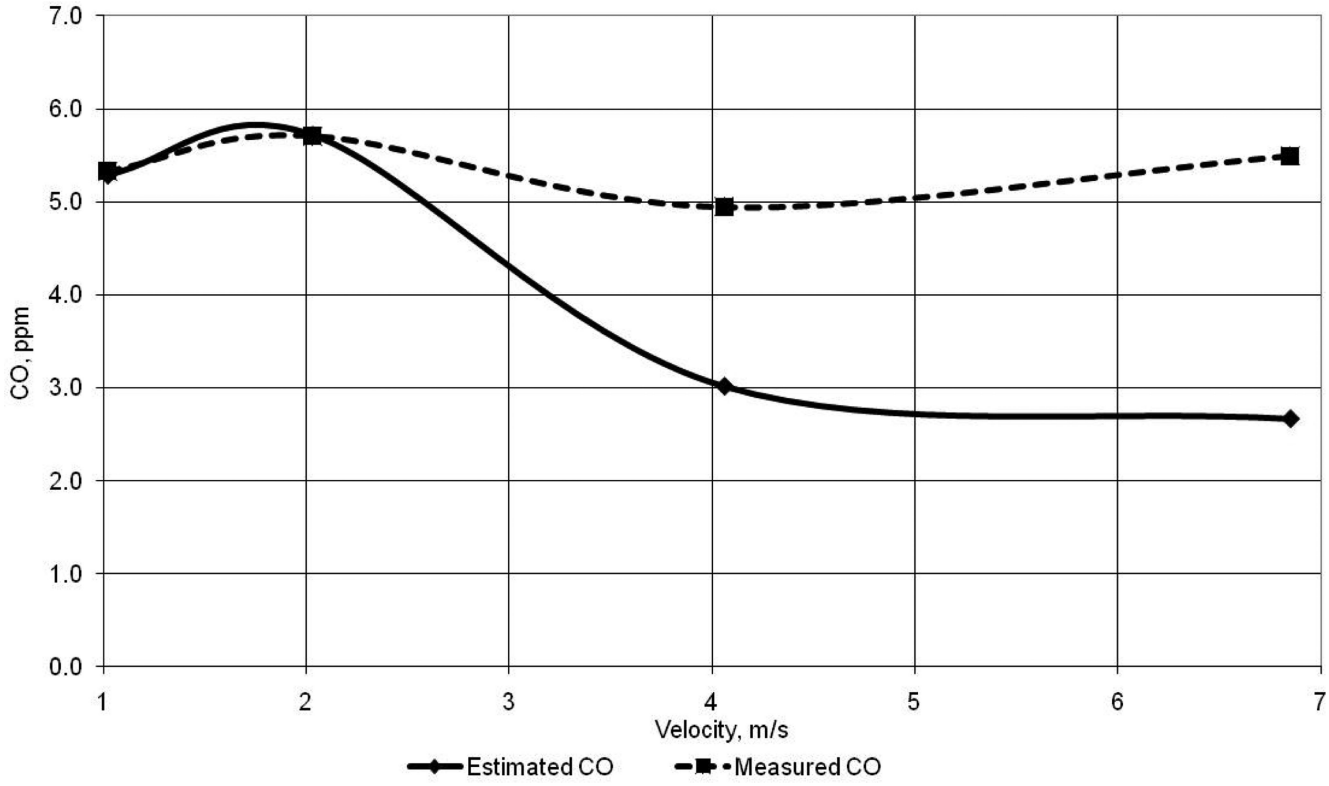

Figure 9.
The average measured CO and average estimated CO at each of the four air velocities used in this study.

Table 1

Estimated CO detection times and the measured times to belt ignition, t_{BI}

Test	Air velocity, m/s	CO alarm, ppm	t_{BI}, mins	Estimated CO alarm, mins
SBR	1.0	9	3.8	8.8
	2.0	5	15.0	18.3
	4.1	3	7.8	8.8
	6.9	3	35.4	57.4
	6.9	1	35.4	35.4
PVC	1.0	9	61.8	69.5
	2.0	5	9.2	7.4
	4.1	3	14.7	14.6
	6.9	3	22.9	21.4
	6.9	1	22.9	-0.4
Neoprene	1.0	9	9.8	16.8
	2.0	5	20.7	27.1
	4.1	3	11.2	10.3
	6.9	3	15.7	21.5
	6.9	1	15.7	5.8

Table 2

Estimated smoke sensor alarm times using the alarms calculated from Ref. 1 and the average measured optical density at smoke alarm

Test	t_{BI}, mins	Alarm OD from nomograph of Ref 1	Smoke alarm time, mins	Smoke alarm time at avg OD=0.0257 m^{-1}
SBR200	3.8	0.044	7.5	−3.0
SBR400	15.0	0.044	18.4	17.1
SBR800	7.8	0.022	6.3	8.3
SBR1350	35.4	0.022	49.8	56.1
PVC200	61.8	0.044	25.2	5.7
PVC400	9.2	0.044	7.8	4.9
PVC800	14.7	0.022	8.8	15.8
PVC1350	22.9	0.022	5.4	9.6
NP200	9.8	0.044	15.2	1.3
NP400	32.7	0.044	27.4	18.8
NP800	16.3	0.022	9.5	10.0
NP1350	20.3	0.022	14.9	18.2

Table 3

Smoke sensor and Axonx alarm times relative to flaming ignition of the coal

Test	Velocity, m/s	Smoke alarm, mins	Axonx alarm, mins
SBR	1.0	−16.8	−15.7
	2.0	−23.8	−26.5
	4.1	−12.3	−16.0
	6.9	NA	NA
PVC	1.0	NA	−9.3
	2.0	5.8	−20.6
	4.1	−7.7	5.3
	6.9	−1.3	−3.9
Neoprene	1.0	17.2	−8.5
	2.0	−3.3	−18.1
	4.1	2.3	−4.2
	6.9	−3.3	9.7

Table 4

Heat release rate and ratio of heat release rate to air velocity at the time of belt ignition and ratio of heat release rate to air velocity at the estimated CO detection time for the twelve experiments in this study

Test	Air velocity, m/s	Q_F at belt ignition, kW	Q_F/V_0 at belt ignition	Q_F/V_0 at CO detection
SBR	1.0	16.3	16.0	20.5
	2.0	38.5	18.9	20.5
	4.1	72.2	17.8	22.6
	6.9	100.0	14.6	18.3
PVC	1.0	NA	NA	NA
	2.0	35.7	17.6	15.5
	4.1	45.4	11.2	11.2
	6.9	NA	NA	NA
Neoprene	1.0	19.8	19.5	23.4
	2.0	47.1	23.2	26.2
	4.1	64.8	15.9	16.4
	6.9	61.9	9.0	10.1

Table 5

Measured CO concentrations compared to the estimated CO concentrations at belt ignition using Equation (1)

Air Velocity, m/s	CO Estimated, ppm	CO measured, ppm	CO Estimated, ppm	CO measured, ppm	CO Estimated, ppm	CO measured, ppm	CO Estimated, ppm	CO measured, ppm
		SBR		PVC		Neoprene		Average
1.0	5.5	5.3	3.7	6.0	6.7	4.7	5.3	5.3
2.0	5.4	3.2	5.1	10.8	6.7	3.2	5.7	5.7
4.1	3.6	3.4	2.3	5.5	3.2	5.9	3.0	4.9
6.9	1.8	1.4	5.1	13.3	1.1	7.8	2.7	5.5

Table 6

CO alarm levels at entry cross sections of 50-90 square feet

Air Quantity Range, cfm (t_D = 14.25 minutes)		CO Alarm Level, ppm	Air Quantity Range, cfm (t_D = 16.24 minutes)		CO Alarm Level, ppm
From	**To**		**From**	**To**	
4500	27413	10	4500	34243	10
27413	31945	9	34243	39445	9
31945	37657	8	39445	45870	8
37657	44895	7	45870	53943	7
44895	54297	6	53943	64203	6
54297	66688	5	64203	77483	5
66688	83465	4	77483	95111	4
83465	107075	3	95111	119489	3
107075	135000	2	119489	135000	2
135000	135000	1	135000	135000	1

Table 7

CO alarm levels at entry cross sections of 80-120 square feet

Air Quantity Range, cfm (t_D = 14.25 minutes)		CO Alarm Level, ppm	Air Quantity Range, cfm (t_D = 16.24 minutes)		CO Alarm Level, ppm
From	**To**		**From**	**To**	
6307	23125	10	6000	30196	10
23125	27561	9	30196	35275	9
27561	33172	8	35737	41741	8
33172	40427	7	41741	50111	7
40427	50210	6	50111	61160	6
50210	63677	5	61160	76116	5
63677	82871	4	76116	96870	4
82871	111287	3	96870	126815	3
111287	156289	2	126815	173128	2
156289	180000	1	173128	180000	1

Table 8

CO alarm levels at entry cross sections of 110-150 square feet

Air Quantity Range, cfm (t_D = 14.25 minutes)		CO Alarm Level, ppm	Air Quantity Range, cfm (t_D = 16.24 minutes)		CO Alarm Level, ppm
From	**To**		**From**	**To**	
9122	18701	10	7500	26531	10
18701	23352	9	26531	31469	9
23352	28907	8	31469	37745	8
28907	36065	7	37745	45965	7
36065	45688	6	45965	57071	6
45688	59340	5	57071	72597	5
59340	79596	4	72597	95145	4
79596	111146	3	95145	129138	3
111146	163678	2	129138	183962	2
163678	225000	1	183962	225000	1

Table 9

CO alarm levels at entry cross sections of 140-180 square feet

Air Quantity Range, cfm (t_D = 14.25 minutes)		CO Alarm Level, ppm	Air Quantity Range, cfm (t_D = 16.24 minutes)		CO Alarm Level, ppm
From	**To**		**From**	**To**	
12301	17974	9	9000	22994	10
17974	24597	8	22994	27978	9
24597	31826	7	27978	34098	8
31826	41342	6	34098	42056	7
41342	54826	5	42056	52912	6
54826	75315	4	52912	68486	5
75315	108595	3	68486	91740	4
108595	166931	2	91740	128406	3
166931	270000	1	128406	190223	2
			190223	270000	1

Table 10

CO alarm levels at entry cross sections of 170-210 square feet

Air Quantity Range, cfm (t_D = 14.25 minutes)		CO Alarm Level, ppm	Air Quantity Range, cfm (t_D = 16.24 minutes)		CO Alarm Level, ppm
From	**To**		**From**	**To**	
12234	27435	7	12245	18449	10
27435	37131	6	18449	24291	9
37131	50491	5	24291	30574	8
50491	70747	4	30574	38405	7
70747	104757	3	38405	49065	6
104757	167313	2	49065	64352	5
167313	300937	1	64352	87694	4
			87694	125868	3
			125868	193174	2
			193174	315000	1

Table 11

CO alarm levels at entry cross sections of 200-240 square feet

Air Quantity Range, cfm (t_D = 14.25 minutes)		CO Alarm Level, ppm	Air Quantity Range, cfm (t_D = 16.24 minutes)		CO Alarm Level, ppm
From	**To**		**From**	**To**	
13110	29217	7	15124	19988	9
29217	39488	6	19988	26812	8
39488	53479	5	26812	34942	7
53479	75044	4	34942	45464	6
75044	111549	3	45464	60392	5
111549	180123	2	60392	83482	4
180123	330040	1	83482	122320	3
			122320	193741	2
			193741	346256	1

Table 12

Smoke alarm levels at entry cross sections of 50-90 square feet

Air Quantity Range, cfm (t_D = 14.25 minutes)		Smoke Alarm Level, OD (m^{-1})	Air Quantity Range, cfm (t_D = 16.24 minutes)		Smoke Alarm Level, OD (m^{-1})
From	**To**		**From**	**To**	
4500	83218	0.044	4500	101110	0.044
83218	120410	0.033	101110	135000	0.033
120410	135000	0.022	135000	135000	0.022

Table 13

Smoke alarm levels at entry cross sections of 80-120 square feet

Air Quantity Range, cfm (t_D = 14.25 minutes)		Smoke Alarm Level, OD (m^{-1})	Air Quantity Range, cfm (t_D = 16.24 minutes)		Smoke Alarm Level, OD (m^{-1})
From	**To**		**From**	**To**	
6000	71473	0.044	6000	90181	0.044
71473	110957	0.033	90181	134814	0.033
110957	180000	0.022	134814	180000	0.022

Table 14

Smoke alarm levels at entry cross sections of 110-150 square feet

Air Quantity Range, cfm (t_D = 14.25 minutes)		Smoke Alarm Level, OD (m^{-1})	Air Quantity Range, cfm (t_D = 16.24 minutes)		Smoke Alarm Level, OD (m^{-1})
From	**To**		**From**	**To**	
7500	61282	0.044	7500	79149	0.044
61282	99119	0.033	79149	124106	0.033
99119	176789	0.022	124106	209639	0.022
176789	225000	0.011	209639	225000	0.011

Table 15

Smoke alarm levels at entry cross sections of 140-180 square feet

Air Quantity Range, cfm (t_D = 14.25 minutes)		Smoke Alarm Level, OD (m^{-1})	Air Quantity Range, cfm (t_D = 16.24 minutes)		Smoke Alarm Level, OD (m^{-1})
From	**To**		**From**	**To**	
9000	53227	0.044	9000	69961	0.044
53227	88121	0.033	69961	112633	0.033
88121	166436	0.022	112633	202221	0.022
166436	270000	0.011	202221	270000	0.011

Table 16

Smoke alarm levels at entry cross sections of 170-210 square feet

Air Quantity Range, cfm (t_D = 14.25 minutes)		Smoke Alarm Level, OD (m^{-1})	Air Quantity Range, cfm (t_D = 16.24 minutes)		Smoke Alarm Level, OD (m^{-1})
From	**To**		**From**	**To**	
10605	46751	0.044	10500	62569	0.044
46751	78729	0.033	62569	102210	0.033
78729	154647	0.022	102210	191834	0.022
154647	315000	0.011	191834	315000	0.011

Table 17

Smoke alarm levels at entry cross sections of 200-240 square feet

Air Quantity Range, cfm (t_D = 14.25 minutes)		Smoke Alarm Level, OD (m^{-1})	Air Quantity Range, cfm (t_D = 16.24 minutes)		Smoke Alarm Level, OD (m^{-1})
From	**To**		**From**	**To**	
13123	41019	0.044	12000	56593	0.044
41019	70970	0.033	56593	93281	0.033
70970	142946	0.022	93281	180363	0.022
142946	360000	0.011	180363	360000	0.011